- 1 Efficacy of chitosan/double-stranded RNA polyplex nanoparticles for gene
- 2 silencing under variable environmental conditions
- 3 Stuart S. Lichtenberg₁, Kanthi Nuti₂, Jason DeRouchey₂, Olga V. Tsyusko₁, and Jason
- 4 M. Unrine₁
- 5 1Department of Plant and Soil Sciences and 2Department of Chemistry, University of
- 6 Kentucky

Abstract

We have investigated the ability of chitosan/double-stranded RNA polyplex nanoparticles to silence genes in *Caenorhabditis elegans* in different environmentally analogous media. Using fluorescence microscopy, we were able to rapidly assess gene knockdown and dsRNA uptake under numerous conditions. Scanning transmission electron micrographs of polyplexes confirms heterogeneous distribution of chitosan and RNA in single particles and a wide range of particle morphologies. High pH and the presence of natural organic matter inhibited the ability of polyplex nanoparticles to silence genes, but were unaffected by the presence of inorganic nitrate and phosphate. Environmental media did not affect particle size in any specific pattern, as determined by dynamic light scattering and fluorescence correlation spectroscopy. The efficacy of polyplexes seems to be closely tied to zeta potential, as all treatments that resulted in a net negative zeta potential (high pH and high natural organic matter) failed to achieve gene knockdown. These results support earlier work that emphasized the importance

of charge in gene carriers and will aid in the development of effective gene silencing biological control agents.

Environmental Significance

When deployed in the field, the structure of RNAi enabled materials will be altered by the environment, and their effectiveness could be compromised under certain conditions. Here, we have explored some of the dominant environmental variables that will affect these materials in an agricultural setting. We have strived to use experimental conditions that mimic realistic exposure scenarios, by using whole organisms and settings that are reasonable approximations of those found in the field. This information will be used to develop materials that retain activity in a broad range of environments and will further the development of safe and effective RNAi technologies.

Introduction

RNA interference (RNAi) is an endogenous cellular process that utilizes double-stranded RNA (dsRNA) as a template for the degradation of a homologous messenger RNA (mRNA)1. Though believed to have evolved as a mechanism for viral defense2 and gene regulation3, RNAi has found immense utility as a functional genomics tool4, and has recently emerged as a promising means of crop protection5. When used as a pest control agent, an insect pest consumes dsRNA that targets an essential gene, resulting in mortality. A key advantage of RNAi compared to small molecule pesticides is specificity. For RNAi to function, the ingested dsRNA must be nearly identical to the target mRNA, restricting a properly designed dsRNA to activity in only a handful of closely related species6. While developed initially for control of insect pest of crops,

RNAi can be used to address invasive forest insects, human disease vectors, and plant parasitic nematodes9. The first commercially available agricultural product using an RNAi construct is a transgenic corn line 10, expected to reach the market prior to 2020, and proof-of-concept studies exist for other crop species as well₁₁. In the prior example, a host crop species is transformed with a transgenic construct that encodes a dsRNA specific to a major pest. Though seemingly simple and elegant in execution, immense investments of both capital and labor are required for the development of transgenic crops, and the regulatory and social hurdles for the adoption of these crops are limit their use to specific countries. Further, the precise specificity of RNAi means that new constructs must be generated for each target species, and new lines generated for each crop bearing the transgene. Transgene constructs will likely remain the preferred method of RNAi delivery for crop species, but key advantages exist for the use of *in-vitro* synthesized dsRNA as pest control agents. These methods will enable the use of RNAi-based biological control agents on crop species unamenable to transformation, and also allow for the targeting of numerous pests without the development of new transgenic strains. In spite of this flexibility, it seems highly unlikely that in-vitro synthesized dsRNA alone, commonly referred to as naked dsRNA, will see much application in agricultural settings. dsRNA is known to degrade extremely rapidly in the environment₁₂, and is poorly assimilated and rapidly degraded by many destructive insect species 13. These deficits represent an enormous barrier to the widespread adoption of *in-vitro* RNAi technologies. However, solutions to these problems are a ripe and active area of research. A wealth of work in this area has already been conducted in the context of therapeutic RNAi, and many of these solutions

44

45

46

47

48

49

50

51

52

53

54

55

56

57

58

59

60

61

62

63

64

65

can be applied to the context of agricultural RNAi as well. A frequently employed method to overcome these limitations is complexation of dsRNA with a nanocarrier. The nanocarrier serves to protect dsRNA from nucleases14, and can alter the mechanisms by which dsRNA is assimilated into cells15. In spite of this interest, there is a dearth of studies that have investigated the role of environment on the efficacy of gene silencing nanomaterials. Many studies have investigated the role of nanomaterial structure and physical properties on cellular uptake16,17, but these are mostly conducted using cell culture methods with an emphasis toward therapeutic ends. Further, the vast majority of research on agricultural RNAi has focused upon the development of knockdown targets18-20, rather than delivery improvement. In an agricultural setting, delivery of dsRNA will be dependent not only on the cellular process of the target organism, but also on environmental interactions prior to ingestion. These interactions have been poorly studied.

In order to address this lack of knowledge, we have developed the following study of the efficacy of chitosan/dsRNA polyplex nanoparticles under differing environmental conditions, using a soil-dwelling model organism, *Caenorhabditis elegans*. In studying RNAi, *C. elegans* possesses a unique set of characteristics that make it the ideal organism for both cellular processes and environmental studies related to RNAi. *C. elegans* is the first organism in which RNAi was described 1 and, consequently, possesses the most detailed descriptions of RNAi cellular mechanisms21-23 and uptake24-26. In addition to this, RNAi response in *C. elegans* can be triggered by oral ingestion of dsRNA27. This allows for the development of a feeding assay that is an approximation of field conditions to be encountered in agricultural settings. Finally,

thanks to the abundance of transgenic strains of *C. elegans* available, we are able to target green fluorescent protein (GFP) to allow rapid, objective assessment of RNAi efficacy.

Of the classes of materials suitable for complexation with dsRNA, among the most studied and most promising are polycationic polymers₂₈₋₃₀. In this particular model, the anionic phosphate backbone of dsRNA has an electrostatic interaction with the cationic groups of the polymer. Under conditions specific to each system, this interaction results in the formation of stable polyplex nanoparticles (PNs). A vast amount of research has been conducted on polycation/nucleic acid complexes, in a search for high efficiency₃₁₋₃₃ and low toxicity₃₄₋₃₆ therapeutics. Chitosan (poly β-1,4-D-glucosamine) in particular has been the subject of much investigation, owing to its inexpensive manufacture from marine waste₃₇, low toxicity₃₈, and wide variety of molecular weights and modifications available₃₉. Several chitosan-based materials for gene silencing have already been tested in insect species_{40,41}, and applications of chitosan in other areas of agricultural management have been identified₄₂₋₄₄.

In our recent work, we discovered several characteristics of chitosan/dsRNA PNs that were previously unknown. Principally, we found that in C. elegans, chitosan/dsRNA PNs are more potent than naked dsRNA on a whole body concentration basis, and that these particles are assimilated outside the canonical dsRNA uptake pathway₁₅. To expand upon this work, we have investigated the efficacy of chitosan/dsRNA PNs while altering environmental variables. We exposed *C. elegans* to chitosan/dsRNA PNs while altering pH, competitive anions (nitrate and phosphate), and natural organic matter (NOM) content in exposure solutions. We selected concentrations of these constituents

that are possible in an agricultural setting to preserve a realistic exposure scenario as closely as possible₄₅₋₄₇. Subsequently, we characterized some of the physical changes that occur in chitosan/dsRNA PNs under these varying conditions, in an attempt to correlate environment, nanomaterial structure, and gene silencing. We hypothesized that as we increased pH, the efficacy of PNs would decline, due to aggregation.

Similarly, we expected that competitive anions would occupy binding sites on cationic chitosan, and eventually displace the dsRNA as well, leading to a reduction in effectiveness. Given the highly negative charge of NOM, we speculated that PNs would be sequestered and rendered unavailable to *C. elegans*, completely eliminating efficacy as NOM concentration increases.

Methods

C. elegans Maintenance

C. elegans strains N2 and CGC4 (umnTi1 III [eft-3p::GFP + unc-119(+)]) were maintained on K-medium agar plates seeded with OP50 Escherichia coli at 20°C, according to established methods₄₈. CGC4 is a transgenic strain produced using the MosSCI system₄₉, which possesses a single copy of GFP at a known location in the genome, driven by a translation elongation promoter eft-3p₅₀. Animals were cared for in in accordance with the University of Kentucky Animal Care and Use Committee, which does not specify any standards for the care of invertebrates as it is not regulated under U.S. Law.

135

136

137

138

139

140

141

142

143

144

145

146

147

148

149

150

151

152

153

154

155

Genomic DNA was isolated from *C. elegans* using phenol-chloroform and ethanol precipitation using established methods 51. Templates for dsRNA synthesis were generated from genomic DNA using PCR by including primers with an appended T7 promoter sequence₅₁ (**Table S1**). Templates were purified using a Qiagen PCR Cleanup Kit (28104, Germantown, MD, USA), and eluted in 18.2 M Ω H₂O (DI). dsRNA was generated using a ThermoFisher Scientific TranscriptAid T7 High Yield Transcription Kit (K0441, Waltham, MA, USA) according to the manufacturer's instructions, and purified using phenol-chloroform followed by ethanol precipitation51 and resuspension in DI. To prepare Alexa Fluor 488 labeled dsRNA, dsRNA was synthesized as above, with the addition of 5-(3-aminoallyl)-UTP (ThermoFisher Scientific AM8437, Waltham, MA, USA) as per the manufacturer's instructions. Aminoallyl-dsRNA was labeled using Alexa Fluor 488 NHS Ester (ThermoFisher Scientific A20000, Waltham, MA, USA), according to the manufacturer's protocol. Labeled dsRNA was separated from unreacted fluorophore using size exclusion chromatography spin columns (BioRad 7326223, Hercules, CA, USA). Reaction yield was confirmed by measuring absorbance at 260 nm using a Varian Cary 50 Bio UV-Vis Spectrophotometer equipped with a Hëllma TrayCell (Hëllma USA, Plainview, NY USA). Typically, a single reaction would yield 150 µg of dsRNA. Polyplexes were prepared using our previously described method₁₅, itself a modification of the Zhang method₄₀. A 0.58% solution of low molecular weight chitosan (Polysciences 21161, Warrington, PA, USA) was prepared in 0.2 M acetate buffer at pH 4.5. dsRNA was diluted to 1 µg/µL in 50 mM Na₂SO₄, and combined with an equal volume of chitosan solution by pipetting.

The solution was then immediately heated in a water bath at 55°C for 1 minute, and then vigorously vortexed for 30 seconds, resulting in the formation of polyplex nanoparticles.

Transmission Electron Microscopy

Samples were prepared by diluting chitosan/dsRNA polyplex to ~50 mg/L in unamended MHRW52. Copper grids coated with lacey formvar/carbon (Ted Pella 01883-F, Redding, CA, USA) were then dipped in the sample, and dried overnight in a desiccator. Electron micrographs were captured using a ThermoFisher Scientific Talos F200X S/TEM with a field emission gun operating at 200 keV, and a Ceta 16 megapixel CCD sensor. Energy-dispersive X-ray spectroscopy mapping was performed in STEM mode, using the Super-X EDS system.

Exposure Media Preparation

For all exposures, the base medium was moderately hard reconstituted water (MHRW)₅₂. For exposures where pH was the independent variable, MHRW was supplemented with 1 mM MES and 1 mM MOPS and the pH was adjusted with sulfuric acid (pH 5, 6, and 7) or sodium hydroxide (pH 8). For nitrate and phosphate MHRW solutions, exposure solutions were prepared with 1 M stock solutions of sodium nitrate or monobasic sodium phosphate, and the pH was subsequently adjusted to 6 with sulfuric acid. Solutions were prepared such that the final concentration indicated in results would be present following addition of polyplex and nematodes. Natural organic matter solutions were prepared similarly, from a 500 mg/L stock solution of Pahokee

peat humic acid (PPHA; International Humic Substances Society, St. Paul, MN, USA), with a subsequent adjustment of the pH to 6 with sulfuric acid.

Polyplex Exposures and Imaging

177

178

179

180

181

182

183

184

185

186

187

188

189

190

191

192

193

194

195

196

197

198

199

Caenorhabditis elegans were age synchronized using sodium hydroxide and sodium hypochlorite according to established methods₄₈, and allowed to hatch on OP50 E. coli seeded K-medium agar plates. After 24 hours, young nematodes were washed from plates with K-medium and placed in 15 mL polypropylene centrifuge tubes. Nematodes were then centrifuged at 160 x g, and the supernatant removed. The medium was replaced with a solution of 25% moderately hard reconstituted water (MHRW)₅₂ and 75% K-medium, and incubated at 20°C for 15 minutes. This process was repeated three additional times, with 25% stepwise increases of MHRW concentration until the final concentration was 100% MHRW. For exposures, 2 µL of compact nematode pellet (~50 worms) was placed in 0.2 mL PCR tubes containing the indicated exposure medium and 100 ng/µL dsRNA as either naked dsRNA or chitosan/dsRNA PN, to a total volume of 20 µL. Control exposures were simultaneously conducted using DI in lieu of dsRNA. All exposures were conducted in triplicate. Tubes with nematodes and exposure medium were then incubated for 24 hours at 20°C. For imaging, an 8 µL drop of exposure media and nematodes was placed on a microscope slide. Nematodes were then anesthetized with 2 µL 50 mM levamisole and secured with a coverslip. Imaging was performed using a Nikon Eclipse 90i microscope equipped with Nikon Intensilight C-HGFI Epifluorescence Illuminator, a Nikon GFP filter cube, and a Nikon DS-Qi1Mc camera (Tokyo, Japan). Multichannel images of individual nematodes were taken at 20x magnification, consisting of DIC (autoexposure) and fluorescence (5s exposure) images. Five nematodes were imaged per exposure replicate. The generated images were then processed using the image analysis software Fiji53. First, the background was subtracted from the GFP channel of each image using the rolling ball method with a radius of 50 pixels. Next, a region of interest was drawn around each nematode using the DIC image, and the mean pixel intensity was measured. The mean pixel intensity of five nematodes was averaged per replicate, and the mean of the replicates is the reported pixel intensity.

Dynamic Light Scattering, Phase Analysis Light Scattering, and Fluorescence Correlation Spectroscopy

Chitosan/dsRNA PNs were prepared as above, using Alexa Fluor 488 labeled dsRNA. Exposure solutions were then prepared using the same indicated environmental variables, replacing the worm pellet volume with MHRW. Samples were then diluted 10X in MHRW with the appropriate indicated amendments.

Dynamic light scattering (DLS) and phase analysis light scattering (PALS) measurements were taken using a Malvern Zetasizer Nano ZS at 25°C, using polystyrene cuvettes for DLS (Malvern Panalytical DTS0012, Westborough, MA, USA) and folded capillary cells for PALS (Malvern Panalytical DTS1070, Westborough, MA, USA). For the PALS measurements, zeta potential is reported using the Hückel approximation.

Fluorescence correlation spectroscopy measurements were taken using an ISS Alba FCS instrument, with a Nikon Eclipse Ti-U inverted confocal microscope and a PlanAPO 1.2 NA 60X water immersion objective serving as the optical apparatus. The laser intensity (488 nm) and pinholes (50 µm) were calibrated using Rhodamine 110

dye in water. Data was collected using the ISS VistaVision software package. The diffusion coefficient was derived from the autocorrelation function of each sample 54, and the hydrodynamic diameter was calculated using the Stokes-Einstein equation 55.

Statistical Analysis

Comparisons between treatments in *C. elegans* experiments, DLS, FCS, and zeta potential measurements were conducted using PROC GLM in SAS 9.4. The Student-Newman-Keuls procedure with α =0.1 was used as a post-hoc test for multiple comparisons.

231 Results

232 Transmission Electron Microscopy

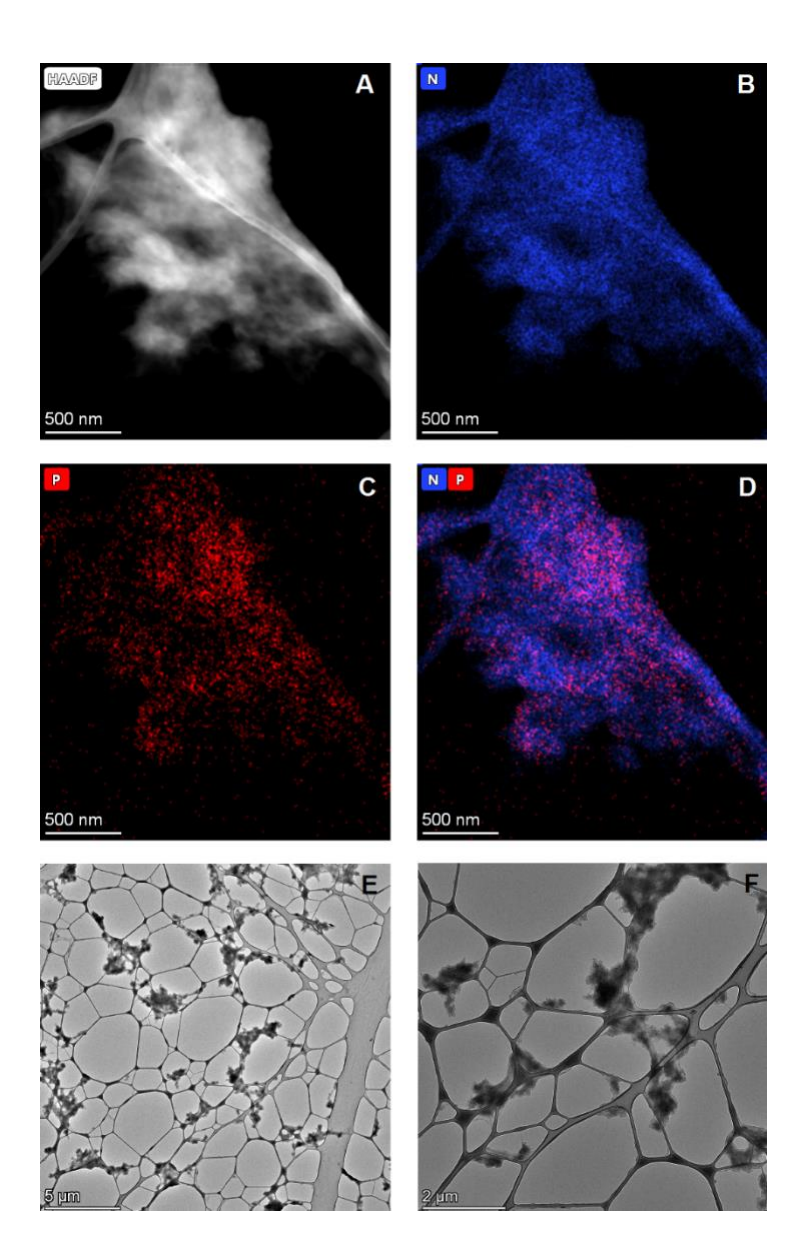


Figure 1 – Energy-dispersive X-ray Spectroscopy (EDS) maps and bright-field images of chitosan/dsRNA polyplex nanoparticles. A – High angle annular dark field image of a chitosan/dsRNA polyplex nanoparticle aggregate, operating in STEM mode. B – EDS map of nitrogen localization. C – EDS map of phosphorus localization. D – Merged EDS mapping of nitrogen and phosphorus localization. E, F – Bright-field images of chitosan/dsRNA polyplex nanoparticles and aggregates.

There is broad colocalization of nitrogen and phosphorus within the chitosan/dsRNA PN (Fig. 1), suggesting that what is shown is indeed a polyplex nanoparticle composed of dsRNA and chitosan. High concentrations of oxygen and carbon are also present within the particle, as would be expected of a polysaccharide based material (Fig. 1). In general, the materials present appear to be composed of small, primary particles, and larger aggregates of these particles, though this distinction can be difficult to discern given the inhomogeneous nature of the particles in general. This is reflected in the wide distribution of particle sizes and morphologies present in the solution, with diameters ranging from ~100-300 nm for individual particles, and 1-2 um for aggregates. The morphologies range from nearly spherical to more amorphous and globular (Fig. 1E, 1F).

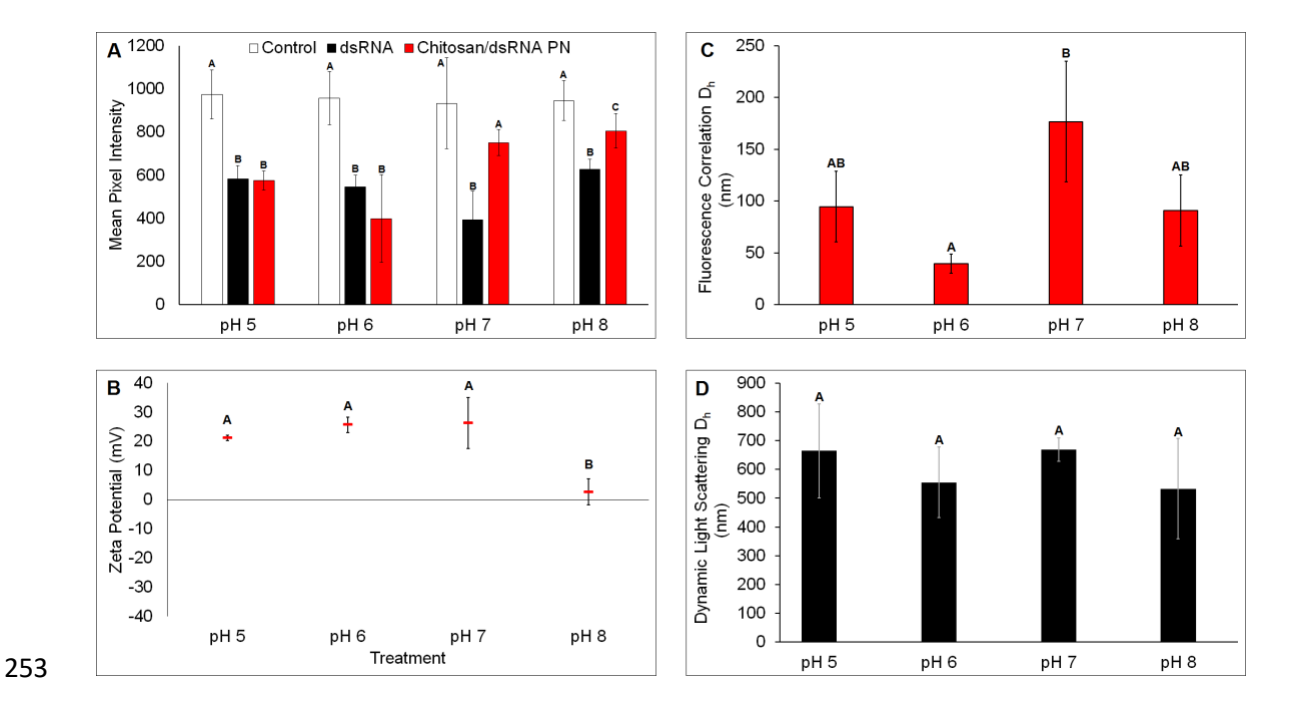


Figure 2 – Gene expression knockdown (as measured by GFP fluorescence intensity) and physical properties of chitosan/dsRNA polyplex nanoparticles under varying pH conditions in moderately hard reconstituted water. Treatments with the same letter are not statistically different (n = 3, α < 0.1). A – Mean fluorescence of CGC4 Caenorhabditis elegans exposed to 100 ng/μL chitosan/dsRNA polyplexes and dsRNA under varying pH. Values represent the mean of 5 nematodes in individual exposure groups. B – Zeta potential of chitosan/dsRNA polyplexes under varying pH. C – Mass weighted hydrodynamic diameter (Dh) of chitosan/dsRNA polyplexes as determined by fluorescence correlation spectroscopy. D – Intensity weighted Z-Average hydrodynamic diameter of chitosan/dsRNA polyplexes as determined by dynamic light scattering.

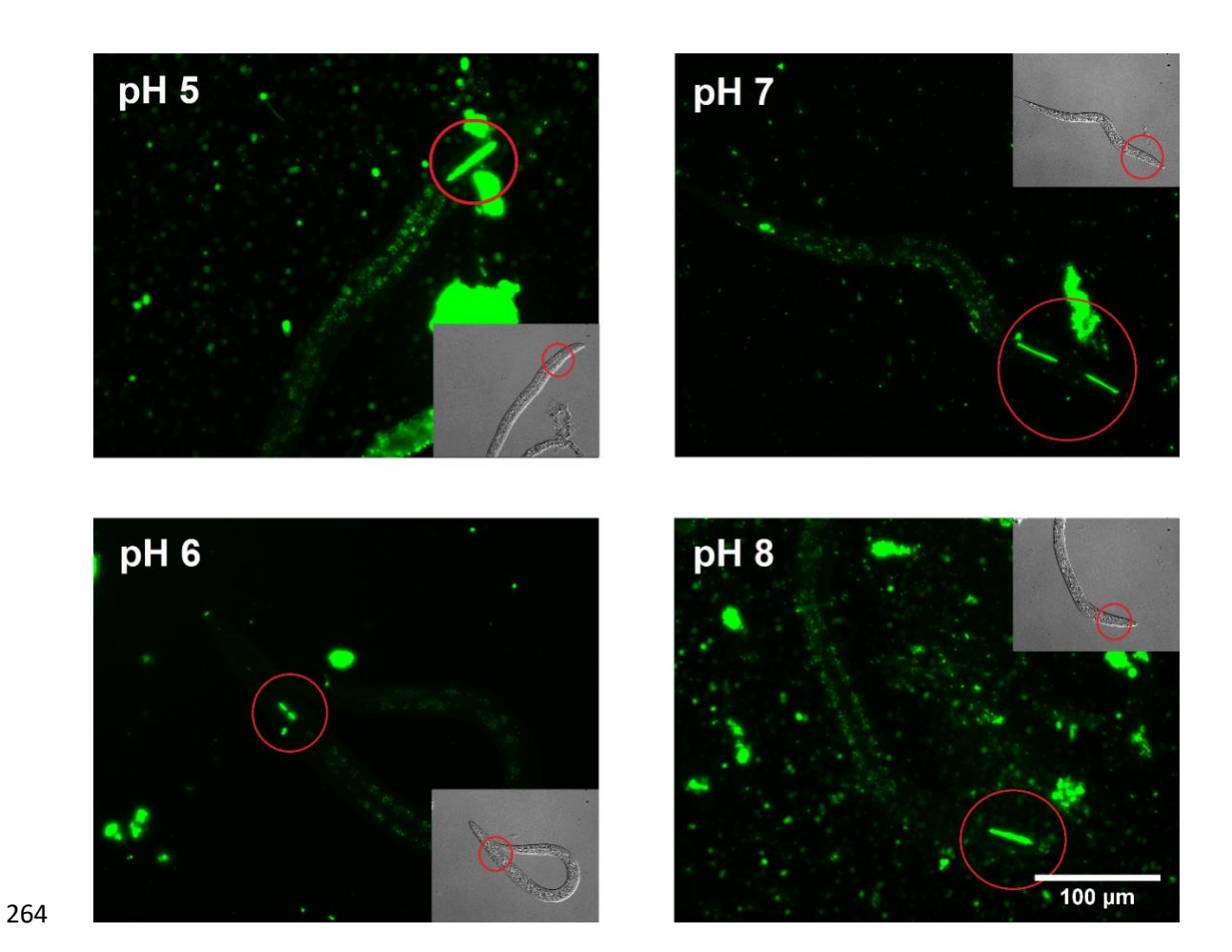


Figure 3 - N2 *Caenorhabditis elegans* exposed to 100 ng/μL chitosan/Alexa Fluor 488 labeled dsRNA polyplex nanoparticles under varying pH conditions. Insets are differential interference contrast (DIC) images of the corresponding fluorescent channel. Areas showing ingestion of polyplex nanoparticles are circled in red.

271

The pH value of the medium influences the efficacy of chitosan/dsRNA PNs. In every exposure scenario, naked dsRNA is effective at gene knockdown (Fig. 2A). At pH 5 and 6, chitosan/dsRNA PNs are equally effective as naked dsRNA at gene knockdown, a result consistent with our earlier work. At pH ≥7, the efficacy of PNs for gene knockdown declines (Fig. 2A). Zeta potential measurements show that chitosan/dsRNA PNs possess a positive zeta potential at pH ≤ 6, positive but increasingly variable at pH 7, and are nominally uncharged at pH 8 (Fig. 2B). DLS measurements of chitosan/dsRNA PN hydrodynamic diameters range from 500-650 nm (Fig. 2D), with no statistical difference among the treatments. The particle diameter measured using FCS was much smaller than with DLS (Fig. 2C), though this is to be expected given that FCS measurements are by definition mass weighted 54 and our reported DLS measurements are intensity weighted 56. Some differences in particle size are present between treatments. There is a statistical difference between the pH 6 samples and the pH 7 samples, though this can largely be accounted for the high degree of variability in the pH 7 treatment. In spite of these differences, the overall difference between particle diameters is comparatively small, with the mean of all treatments falling between 50 and 150 nm. In all treatments, there is evidence that the fluorescently labeled chitosan/dsRNA PNs are ingested by *C. elegans* (Fig. 3).

288

Influence of inorganic anions on chitosan/dsRNA polyplex nanoparticle bioactivity

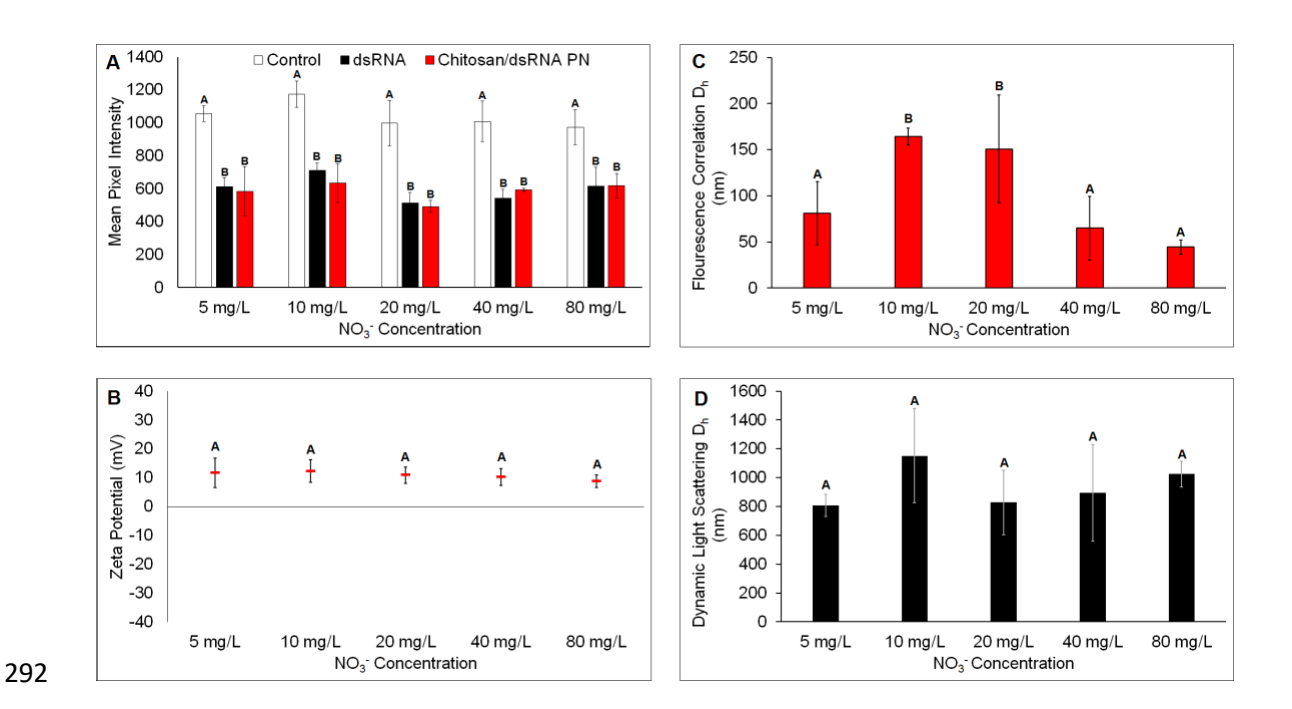


Figure 4 - Gene expression knockdown (as measured by GFP fluorescence intensity) and physical properties of chitosan/dsRNA polyplex nanoparticles under varying inorganic nitrate concentrations in moderately hard reconstituted water. Treatments with the same letter are not statistically different (n = 3, α < 0.1). A – Mean fluorescence of CGC4 *Caenorhabditis elegans* exposed to 100 ng/μL chitosan/dsRNA polyplexes and dsRNA under varying phosphate concentrations. Values represent the mean of 5 nematodes in individual exposure groups. B – Zeta potential of chitosan/dsRNA PN under varying phosphate concentrations. C – Mass weighted hydrodynamic diameter (Dh) of chitosan/dsRNA polyplexes as determined by fluorescence correlation spectroscopy. D – Intensity weighted Z-Average hydrodynamic diameter of chitosan/dsRNA polyplexes as determined by dynamic light scattering.

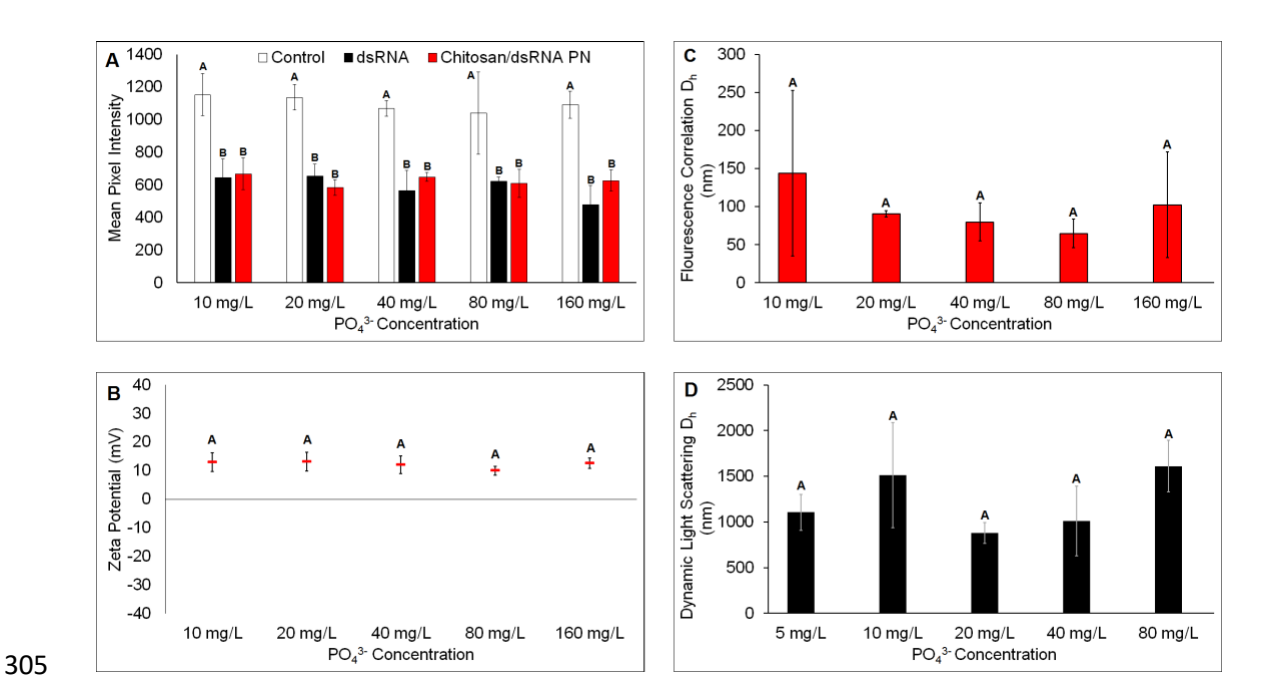


Figure 5 - Gene expression knockdown (as measured by GFP fluorescence intensity) and physical properties of chitosan/dsRNA polyplex nanoparticles under varying inorganic phosphate concentrations in moderately hard reconstituted water. Treatments with the same letter are not statistically different (n = 3, α < 0.1). A – Mean fluorescence of CGC4 *Caenorhabditis elegans* exposed to 100 ng/μL chitosan/dsRNA polyplexes and dsRNA under varying nitrate concentrations. Values represent the mean of 5 nematodes in individual exposure groups. B – Zeta potential of chitosan/dsRNA polyplexes under varying nitrate concentrations. C – Mass weighted hydrodynamic diameter (Dh) of chitosan/dsRNA polyplexes as determined by fluorescence correlation spectroscopy. D – Intensity weighted Z-Average hydrodynamic diameter of chitosan/dsRNA polyplexes as determined by dynamic light scattering.

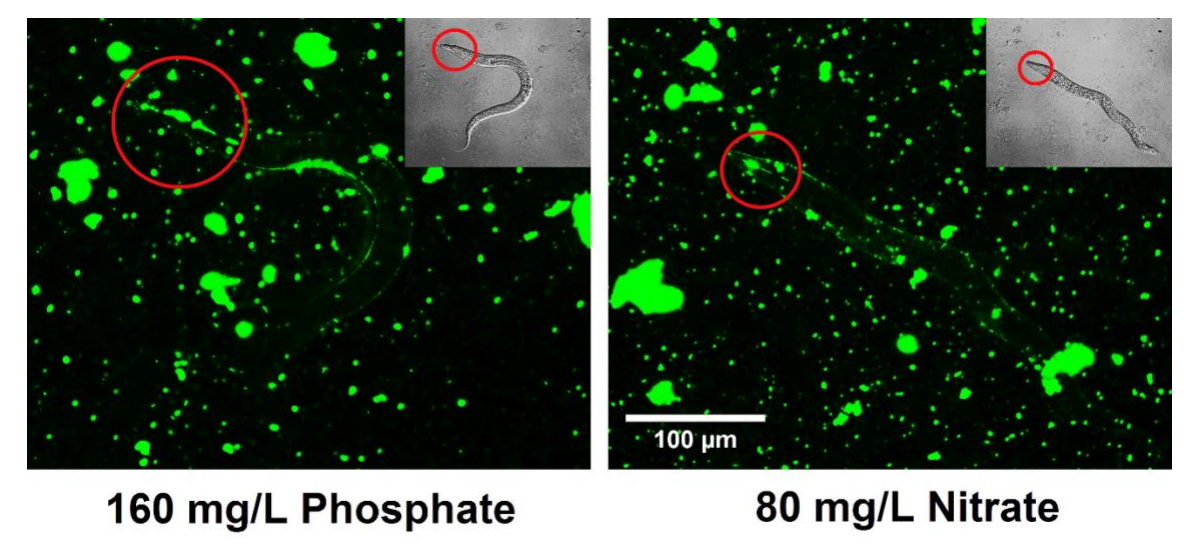
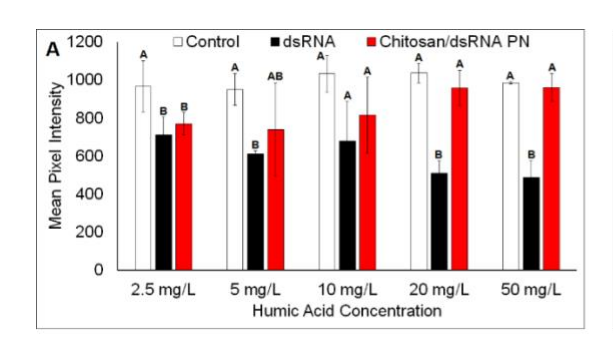
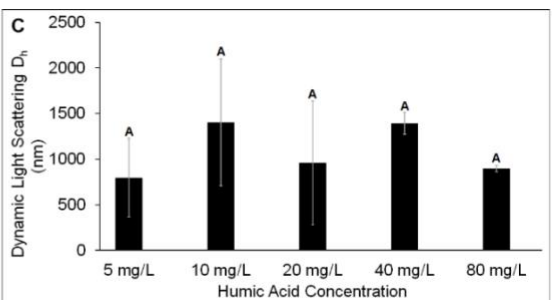


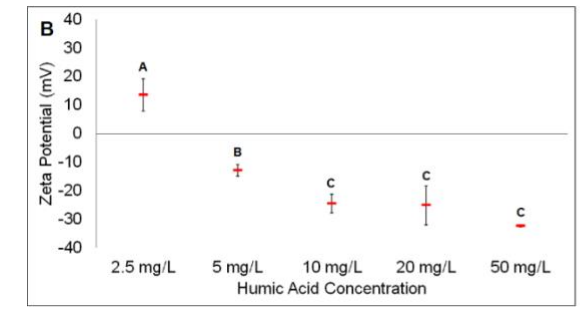
Figure 6 - N2 *Caenorhabditis elegans* exposed to 100 ng/μL chitosan/Alexa Fluor 488 labeled dsRNA polyplex nanoparticles at the maximum phosphate and nitrate conditions. Insets are differential interference contrast (DIC) images of the corresponding fluorescent channel. Areas showing ingestion of polyplex nanoparticles are circled in red.

None of the experiments where inorganic phosphate and nitrate were varied resulted in a failure of knockdown for either naked dsRNA or chitosan/dsRNA PNs (Fig. 4A, 5A). Hydrodynamic diameter measurements by FCS show that particles in all treatments are approximately the same size, on the order of 100-150 nm (Fig. 4C, 5C). Though there are some differences in the hydrodynamic diameter of PNs 10 mg/L and 20 mg/L NO₃ treatments, the magnitude of these differences is small. Hydrodynamic diameter measurements by DLS were similar, in that particles were roughly the same diameter within treatments (Fig. 4D, 5D). Zeta potential is substantially reduced compared to the low pH samples (Fig 4B, 5B, 2B), but is still positive. Fluorescence imaging with chitosan/Alexa Fluor 488 labeled dsRNA PNs at the highest concentrations of phosphate and nitrate (Fig. 6) clearly shows that in both cases, PNs are internalized by *C. elegans*.

Influence of Natural Organic Matter on chitosan/dsRNA polyplex nanoparticle bioactivity







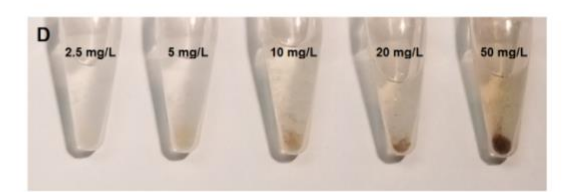


Figure 7 - Gene expression knockdown (as measured by GFP fluorescence intensity) and physical properties of chitosan/dsRNA polyplex nanoparticles under varying humic acid concentrations in moderately hard reconstituted water. Treatments with the same letter are not statistically different (n = 3, α < 0.1). A – Mean fluorescence of CGC4 Caenorhabditis elegans exposed to 100 ng/ μ L chitosan/dsRNA polyplexes and dsRNA under varying natural organic matter concentrations. Values represent the mean of 5 nematodes in individual exposure groups. B – Zeta potential of chitosan/dsRNA polyplexes under varying natural organic matter concentrations. C – Intensity weighted Z-Average hydrodynamic diameter (Dh) of chitosan/dsRNA polyplexes as determined by dynamic light scattering. D – Visible aggregates present in the humic acid/polyplex solutions.

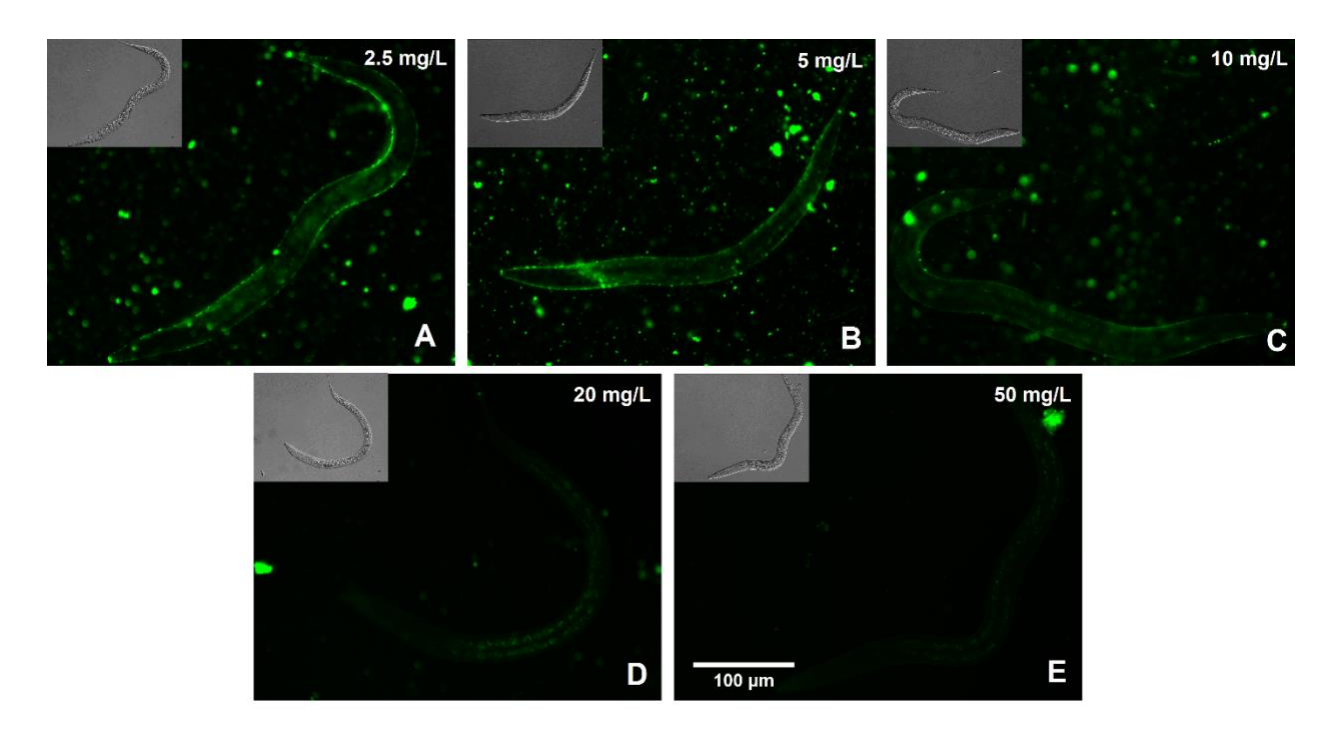


Figure 8 - N2 *Caenorhabditis elegans* exposed to 100 ng/μL chitosan/Alexa Fluor 488 labeled dsRNA polyplex nanoparticles and Pahokee peat humic acid. Insets are differential interference contrast (DIC) images of the corresponding fluorescent channel. A – 2.5 mg/L humic acid; B – 5 mg/L humic acid; C – 10 mg/L humic acid; D – 20 mg/L humic acid; E – 50 mg/L humic acid

353

354

355

356

357

358

359

360

361

362

363

364

365

366

367

368

369

370

371

372

373

374

375

As in the previous experiments, no treatment level of NOM affected gene knockdown by naked dsRNA (Fig. 7A). At low concentrations ($\leq 2.5 \text{ mg/L}$) of NOM (Fig. 7A), chitosan/dsRNA PNs are effective. However, at all concentrations tested beyond that, knockdown is absent and PN treatments are statistically indistinguishable from controls. As with all previously discussed experiments, particle size does not appear to be a factor in knockdown efficacy (Fig. 7C), though we are only able to estimate size from DLS, since fluorescence from NOM complicated FCS measurments₅₇. Between concentrations of 2.5 and 5 mg/L, there is a charge reversal, from positive to negative, in the zeta potential measurements (Fig. 7B). We also observe the presence of large aggregates in each of the samples that are visible to the naked eye (Fig. 7D). As the concentration of humic acid increases, so does the coloration of the aggregates. At low concentrations of humic acid, images using chitosan/Alexa Fluor 488 dsRNA PNs are similar to those in other, effective exposures (Fig. 8A, 8B, 8C), though we were unable to find evidence of internalized PNs. PNs still adhere to the *C. elegans* cuticle. It is worth noting that high concentrations of humic acid complicate fluorescence microscopy due to quenching, as determined by our own observations (Fig. S3) and those of others 58, 59. However, the quenching we observed was moderate (Fig. S3).

Discussion

The principal aim of this study was to characterize the ability of chitosan/dsRNA PNs to silence genes under different chemical conditions. Of our tested conditions, high pH and modest concentrations of natural organic matter impede PN efficacy. PN efficacy is unaffected by anion concentration or low pH. Initially, we believed there were several different phenomena that could explain a lack of chitosan/dsRNA PN efficacy for any given treatment. One possibility we thought highly likely is that the particles are unstable at high pH or ionic strength and may aggregate to the extent that they are unavailable to *C. elegans*. The adult *C. elegans* pharynx is estimated to be approximately 1 μm in diameter, but can stretch to allow passage of larger particles, on the order of 4-5 μm₆₀. It is quite clear from fluorescence imaging and hydrodynamic diameter measurements that this is not a likely explanation for samples which did not show gene knockdown, in the case of the pH exposures.

The FCS measurements found a much smaller hydrodynamic diameter than the DLS measurements. This is expected, since DLS is based on fluctuations in scattered light and FCS is based on fluctuations of fluorescence of the particles. Scattering of light dramatically increases with the radius of the particle (related to the r₆), thus in DLS, the presence of a few large particles greatly increases the intensity weighted average hydrodynamic diameter. The FCS measurements do not have this bias as particles are represented based on the amount of fluorescent label in the particles which is related to particle mass. At pH 8, the FCS measurement showed an increase in particle size

while the DLS measurement didn't. This could be attributable to a lower isoelectric point of dsRNA-chitosan PNs relative to chitosan only particles. If this were the case, the PNs would aggregate at pH 8, but not the chitosan only particles. This would be consistent with the observed differences between the FCS and DLS data, since FCS only detects particles containing the fluorescently labelled dsRNA.

Our fluorescence microscopy studies clearly show that *C. elegans* are capable of internalizing chitosan/dsRNA PNs under all of the studied pH conditions. Also, the *C. elegans* gut is consistently acidic₆₁, which would imply that PNs have a similar positive charge while passing the digestive tract. However, if dsRNA desorbs from the chitosan in the medium, as suggested by FCS and DLS data, then one would expect the efficacy of the dsRNA to decrease given that the chitosan/dsRNA PN is more effective at gene knockdown than naked dsRNA.

The driver of gene silencing failure in our NOM experiments is likely interactions between cationic chitosan and anionic humic acid, through aggregation and removal of PNs. Under native synthesis conditions, chitosan/dsRNA PNs possess a positive zeta potential. An abundance of chitosan (pKa 6.5)62 at the particle surface, as observed in our STEM elemental mapping, would account for the highly positive zeta potential of chitosan/dsRNA PNs at pH < 6, and also the reduction of zeta potential as pH increases. Interactions between polyplex surfaces and organic matter would be expected and could cause neutralization of the positive charge and bridging between particles leading to extensive aggregation. We have previously observed that NOM causes aggregation and decreased uptake of positively charged diethylaminoethyldextran coated CeO2 particles in *C. elegans*63. This is evidenced by

the charge reversal observed above 2.5 mg humic acid/L. This is confirmed in our fluorescence imaging studies with humic acid, where at 20 mg/L and higher, only large aggregates are present in solution. Previous studies that have investigated the effects of natural organic matter on nanoparticle-biota interactions have generally found that biological effects such as toxicity_{63, 64} tend to be decreased by the presence of NOM. From this study, it is clear that this phenomenon is true for cationic PNs as well.

Notably, naked dsRNA effectively silences genes in most of the exposure scenarios we investigated, with some variability at various concentrations. The phosphate backbone of dsRNA gives it an essentially permanent anionic character, which would limit interactions with NOM and inorganic anions. Though dsRNA specific transporters are known to have a pH dependence for effective binding of substrates65, the pH of the *C. elegans* gut is tightly regulated, as discussed earlier, thus accounting for the lack of any change in gene silencing based upon exposure media pH.

Conclusions

In this work, we have identified factors that will likely play into the efficacy of chitosan-dsRNA PNs in agricultural settings. We conclude that is unlikely that inorganic ions will influence stability, degradation, or bioactivity of such materials. Rather, environmental pH and interactions with substrates such as natural organic matter will be the dominant factors that must be considered. Through the use of higher pKa polymers, it is quite possible that inactivity due to high pH could be avoided, though this will need to be balanced with the increased toxicity associated with most other polycations³⁴. Other means will have to be employed to avoid the much more promiscuous

interactions with natural biomolecules, such as microencapsulation66. Though investigations into gene silencing nanomaterials as biological control agents are comparatively new, we must again stress the importance of realistic exposure scenarios, particularly as it relates to the use of materials that will be employed in the endless complexity of the natural environment.

Acknowledgements

The authors wish to thank S. Shrestha and A. Wamucho for assistance with *C. elegans*. All strains were obtained from the Caenorhabditis Genetics Center, which is funded by NIH Office of Research Infrastructure Programs (P40 OD010440). This material is based upon work supported by the National Science Foundation under Grant No. CBET-1712323 and Cooperative Agreement EF-0830093. Any opinions, findings, and conclusions or recommendations expressed in this material are those of the author(s) and do not necessarily reflect the views of the National Science Foundation. Portions of the work were also supported by the U.S.-Israel Agricultural Research and Development Fund through grant number IS-4964-16 R.

458

443

444

445

446

447

448

449

450

451

452

453

454

455

456

- A. Fire, S. Q. Xu, M. K. Montgomery, S. A. Kostas, S. E. Driver and C. C. Mello, *Nature*, 1998, **391**, 806-811.
- 461 2. S. W. Ding, H. W. Li, R. Lu, F. Li and W. X. Li, Virus Res., 2004, **102**, 109-115.
- 462 3. A. Grishok, A. E. Pasquinelli, D. Conte, N. Li, S. Parrish, I. Ha, D. L. Baillie, A. Fire, G. Ruvkun and C. C. Mello, *Cell*, 2001, **106**, 23-34.
- 464 4. R. S. Kamath, A. G. Fraser, Y. Dong, G. Poulin, R. Durbin, M. Gotta, A. Kanapin, N. Le Bot, S.
- Moreno, M. Sohrmann, D. P. Welchman, P. Zipperlen and J. Ahringer, *Nature*, 2003, **421**, 231-466 237.
- 467 5. F. Zhu, J. J. Xu, R. Palli, J. Ferguson and S. R. Palli, *Pest Manag. Sci.*, 2011, **67**, 175-182.
- 468 6. J. G. Tan, S. L. Levine, P. M. Bachman, P. D. Jensen, G. M. Mueller, J. P. Uffman, C. Meng, Z. H. Song, K. B. Richards and M. H. Beevers, *Environ. Toxicol. Chem.*, 2016, **35**, 287-294.
- 470 7. T. B. Rodrigues, J. J. Duan, S. R. Palli and L. K. Rieske, *Sci Rep*, 2018, **8**, 9.

- 471 8. S. Whyard, C. N. G. Erdelyan, A. L. Partridge, A. D. Singh, N. W. Beebe and R. Capina, *Parasites Vectors*, 2015, **8**, 11.
- 473 9. A. S. Sindhu, T. R. Maier, M. G. Mitchum, R. S. Hussey, E. L. Davis and T. J. Baum, *J. Exp. Bot.*, 2009, **60**, 315-324.
- G. P. Head, M. W. Carroll, S. P. Evans, D. M. Rule, A. R. Willse, T. L. Clark, N. P. Storer, R. D.
 Flannagan, L. W. Samuel and L. J. Meinke, *Pest Manag. Sci.*, 2017, **73**, 1883-1899.
- 477 11. R. X. Ran, T. Y. Li, X. X. Liu, H. J. Ni, W. B. Li and F. L. Meng, *PeerJ*, 2018, **6**, 19.
- 478 12. S. Dubelman, J. Fischer, F. Zapata, K. Huizinga, C. J. Jiang, J. Uffman, S. Levine and D. Carson, *PLoS One*, 2014, **9**, 7.
- 480 13. J. N. Shukla, M. Kalsi, A. Sethi, K. E. Narva, E. Fishilevich, S. Singh, K. Mogilicherla and S. R. Palli, 481 *RNA Biol.*, 2016, **13**, 656-669.
- 482 14. H. Katas, E. Cevher and H. O. Alpara, Int. J. Pharm., 2009, **369**, 144-154.
- 483 15. S. S. Lichtenberg, O. V. Tsyusko, S. R. Palli and J. M. Unrine, *Environ. Sci. Technol.*, 2019, DOI: 10.1021/acs.est.8b06560.
- 485 16. S. L. Zhang, J. Li, G. Lykotrafitis, G. Bao and S. Suresh, *Adv. Mater.*, 2009, **21**, 419-+.
- 486 17. L. A. Chen, J. M. McCrate, J. C. M. Lee and H. Li, *Nanotechnology*, 2011, **22**, 10.
- 487 18. J. Q. Xie, S. J. Li, W. Zhang and Y. X. Xia, *Pest Manag. Sci.*, 2019, **75**, 1383-1390.
- 488 19. M. L. Taracena, C. M. Hunt, M. Q. Benedict, P. M. Pennington and E. M. Dotson, *Parasites Vectors*, 2019, **12**, 11.
- 490 20. K. Tariq, A. Ali, T. G. E. Davies, E. Naz, L. Naz, S. Sohail, M. L. Hou and F. Ullah, *Sci Rep*, 2019, **9**, 8.
- 491 21. H. Tabara, M. Sarkissian, W. G. Kelly, J. Fleenor, A. Grishok, L. Timmons, A. Fire and C. C. Mello, 492 *Cell*, 1999, **99**, 123-132.
- 493 22. T. Sijen, J. Fleenor, F. Simmer, K. L. Thijssen, S. Parrish, L. Timmons, R. H. A. Plasterk and A. Fire, *Cell*, 2001, **107**, 465-476.
- 495
 496
 496
 497
 A. Ashe, A. Sapetschnig, E. M. Weick, J. Mitchell, M. P. Bagijn, A. C. Cording, A. L. Doebley, L. D.
 498
 499
 490
 490
 490
 491
 492
 493
 494
 495
 496
 497
 497
 498
 499
 499
 499
 490
 490
 490
 490
 490
 490
 490
 490
 490
 490
 490
 490
 490
 490
 490
 490
 490
 490
 490
 490
 490
 490
 490
 490
 490
 490
 490
 490
 490
 490
 490
 490
 490
 490
 490
 490
 490
 490
 490
 490
 490
 490
 490
 490
 490
 490
 490
 490
 490
 490
 490
 490
 490
 490
 490
 490
 490
 490
 490
 490
 490
 490
 490
 490
 490
 490
 490
 490
 490
 490
 490
 490
 490
 490
 490
 490
 490
 490
 490
 490
 490
 490
 490
 490
 490
 490
 490
 490
 490
 490
 490
 490
 490
 490
 490
 490
 490
 490
 490
 490
 490
 490
 490
 490
 490
 490
 490
 490
 490
 490
 490
 490
 490
 490
 490
 490
 490
 490
 490
 490
 490
 490
 490
 490
 490
 490
 490
 490
- 498 24. W. M. Winston, C. Molodowitch and C. P. Hunter, *Science*, 2002, **295**, 2456-2459.
- 499 25. W. M. Winston, M. Sutherlin, A. J. Wright, E. H. Feinberg and C. P. Hunter, *Proc. Natl. Acad. Sci.* 500 *U. S. A.*, 2007, **104**, 10565-10570.
- 501 26. A. Hinas, A. J. Wright and C. P. Hunter, *Curr. Biol.*, 2012, **22**, 1938-1943.
- 502 27. J. Ahringer (ed.), *Journal*, DOI: 10.1895/wormbook.1.47.1.
- 503 28. K. Numata, M. Ohtani, T. Yoshizumi, T. Demura and Y. Kodama, *Plant Biotechnol. J.*, 2014, **12**, 504 1027-1034.
- 505 29. J. H. Li, J. Qian, Y. Y. Xu, S. Yang, J. Shen and M. Z. Yin, *ACS Sustain. Chem. Eng.*, 2019, **7**, 6316-6322.
- 507 30. A. Zintchenko, A. Philipp, A. Dehshahri and E. Wagner, *Bioconjugate Chem.*, 2008, **19**, 1448-508 1455.
- 509 31. M. Thomas and A. M. Klibanov, *Proc. Natl. Acad. Sci. U. S. A.*, 2002, **99**, 14640-14645.
- 510 32. M. Thomas, Q. Ge, J. J. Lu, J. Z. Chen and A. M. Klibanov, *Pharm. Res.*, 2005, **22**, 373-380.
- 511 33. L. W. Warriner, J. R. Duke, D. W. Pack and J. E. DeRouchey, *Biomacromolecules*, 2018, **19**, 4348-512 4357.
- 513 34. D. Fischer, Y. X. Li, B. Ahlemeyer, J. Krieglstein and T. Kissel, *Biomaterials*, 2003, **24**, 1121-1131.
- T. Merdan, K. Kunath, H. Petersen, U. Bakowsky, K. H. Voigt, J. Kopecek and T. Kissel,
- 515 *Bioconjugate Chem.*, 2005, **16**, 785-792.
- 516 36. K. Itaka, T. Ishii, Y. Hasegawa and K. Kataoka, *Biomaterials*, 2010, **31**, 3707-3714.
- 37. J. A. Vazquez, I. Rodriguez-Amado, M. I. Montemayor, J. Fraguas, M. D. Gonzalez and M. A.
- 518 Murado, *Mar. Drugs*, 2013, **11**, 747-774.

- 519 38. T. Kean and M. Thanou, *Adv. Drug Deliv. Rev.*, 2010, **62**, 3-11.
- 39. X. D. Liu, K. A. Howard, M. D. Dong, M. O. Andersen, U. L. Rahbek, M. G. Johnsen, O. C. Hansen,
- 521 F. Besenbacher and J. Kjems, *Biomaterials*, 2007, **28**, 1280-1288.
- 522 40. X. Zhang, J. Zhang and K. Y. Zhu, *Insect Mol. Biol.*, 2010, **19**, 683-693.
- 523 41. D. R. Kumar, P. S. Kumar, M. R. Gandhi, N. A. Al-Dhabi, M. G. Paulraj and S. Ignacimuthu, *Int. J.*
- 524 Biol. Macromol., 2016, **86**, 89-95.
- 525 42. M. Bittelli, M. Flury, G. S. Campbell and E. J. Nichols, *Agric. For. Meteorol.*, 2001, **107**, 167-175.
- 43. R. Grillo, A. E. S. Pereira, C. S. Nishisaka, R. de Lima, K. Oehlke, R. Greiner and L. F. Fraceto, *J.*
- 527 *Hazard. Mater.*, 2014, **278**, 163-171.
- 528 44. D. Vandamme, I. Foubert, B. Meesschaert and K. Muylaert, J. Appl. Phycol., 2010, 22, 525-530.
- 529 45. E. E. S. a. K. A. Kelling.
- 530 46. R. F. Spalding and M. E. Exner, J. Environ. Qual., 1993, **22**, 392-402.
- 531 47. R. R. Weil and N. C. Brady, *The nature and properties of soils*, 2016.
- 532 48. S. Brenner, *Genetics*, 1974, **77**, 71-94.
- 533 49. C. Frøkjær-Jensen, M. Wayne Davis, C. E. Hopkins, B. J. Newman, J. M. Thummel, S.-P. Olesen,
- 534 M. Grunnet and E. M. Jorgensen, *Nature Genet.*, 2008, **40**, 1375.
- 535 50. D. D. Shaye and I. Greenwald, *PLoS One*, 2011, **6**, e20085.
- 536 51. M. R. Green and J. Sambrook, *Molecular Cloning: A Laboratory Manual*, Cold Spring Harbor Press, 4th edn., 2012.
- 538 52. C. I. Weber, *Journal*, 2002.
- 539 53. J. Schindelin, I. Arganda-Carreras, E. Frise, V. Kaynig, M. Longair, T. Pietzsch, S. Preibisch, C.
- Rueden, S. Saalfeld, B. Schmid, J.-Y. Tinevez, D. J. White, V. Hartenstein, K. Eliceiri, P. Tomancak and A. Cardona, *Nat Meth*, 2012, **9**, 676-682.
- 542 54. O. Krichevsky and G. Bonnet, Rep. Prog. Phys., 2002, **65**, 251-297.
- 543 55. A. Einstein, *Annalen der Physik*, 1905, **322**, 549-560.
- 544 56. B. J. Berne and R. Pecora, *Dynamic Light Scattering: With Applications to Chemistry, Biology, and Physics*, Dover Publications, 2000.
- 546 57. Lead, Jr., K. J. Wilkinson, K. Starchev, S. Canonica and J. Buffle, *Environ. Sci. Technol.*, 2000, **34**, 1365-1369.
- 548 58. H. Zipper, C. Buta, K. Lammle, H. Brunner, J. Bernhagen and F. Vitzthum, *Nucleic Acids Res.*, 2003, **31**, 16.
- 550 59. M. M. Puchalski, M. J. Morra and R. Vonwandruszka, *Environ. Sci. Technol.*, 1992, **26**, 1787-1792.
- 551 60. L. Avery and B. B. Shtonda, The Journal of experimental biology, 2003, 206, 2441-2457.
- 552 61. V. M. Chauhan, G. Orsi, A. Brown, D. I. Pritchard and J. W. Aylott, *ACS Nano*, 2013, **7**, 5577-5587.
- 553 62. A. K. Singla and M. Chawla, *J. Pharm. Pharmacol.*, 2001, **53**, 1047-1067.
- 554 63. B. Collin, E. Oostveen, O. V. Tsyusko and J. M. Unrine, *Environ. Sci. Technol.*, 2014, **48**, 1280-555 1289.
- 556 64. B. Collin, O. V. Tsyusko, D. L. Starnes and J. M. Unrine, *Environ.-Sci. Nano*, 2016, **3**, 728-736.
- 557 65. D. L. McEwan, A. S. Weisman and C. P. Huntert, *Mol. Cell*, 2012, **47**, 746-754.
- 558 66. C. E. Astete and C. M. Sabliov, J. Biomater. Sci.-Polym. Ed., 2006, 17, 247-289.